STRENGTH OF ADHESIVELY BONDED
SINGLE-STRAPPED JOINTS LOADED IN TENSION

Marin SANDU, Adriana SANDU, Dan Mihai CONSTANTINESCU

University "Politehnica" of Bucharest
E-mail: marin_sandu@yahoo.com

Adhesive bonding has proven to be a very effective method for joining structural components, especially those made from dissimilar materials. If the joint is well designed and correctly executed, the adhesive bond ought to be one of the strongest components of the structure and most certainly should not be the reason for reducing the load capacity or fatigue life. In order to ensure efficiency, safety and reliability of bonded joints an adequate understanding of their behaviour is necessary.This work focuses on the evaluation of the load capacity of some configurations of adhesively bonded single-strapped joints based on analytical pre-dimensioning calculus and nonlinear elastic finite element analyses.

Key words: Adhesive bonding; Single-strapped joints; Nonlinear finite element analysis.

1. INTRODUCTION

Adhesive bonding is a particularly effective method for joining structural components from dissimilar materials [1]. The primary function of an adhesive bonded joint is the transfer of load by shear. However, shear and peel stresses distributions along the adhesive layer are uneven, as the edges will experience the loading peak values, while the central regions will be less affected.

Correct evaluation of in service behaviour of adhesively bonded joints is necessary to ensure the efficiency, safety and reliability of this kind of assembling. While several joint geometries, such as the single- and double-lap joints have gained considerable attention, the single-strap configuration has received little consideration because earlier studies have shown it to be less efficient. However, many recent papers [2–10] have demonstrated that properly designed single-strap joints can be as efficient as lap joints. On the other hand, a good solution as the double-strapped joint is not applicable if the external surface of the structure is required to be smooth. Additionally, in many aircraft, automotive and other repairs the only practical joint configuration is the single-strap joint. Single strapped joints with a large gap between the ends of outer adherends can be designed as to be used as specimen for testing adhesives at combined loading (tension and bending), as is suggested in [3]. The main objective of paper [8] was to contradict the statement that a single-strap joint is less efficient than the single-lap joint. This task was accomplished through a detailed analytical investigation of the joint parameters that govern the peak stresses in the adhesive.

If the outer adherends and the inner adherend (the strap) have the same stiffness, the joint is so-called balanced. In paper [8] the deformations of a typical unbalanced single-strapped joint were determined analytically and subsequently used to calculate the bending moments and the shear forces at the two ends of the overlap, that affect the peak stresses in adhesive. The analytical expressions were then simplified for the case of balanced joints with a long overlap. To solve differential equations that govern the distribution of peel and shear stresses in adhesive, proper boundary and continuity conditions were imposed.

In the case of balanced single-strapped joint, closed-form solutions were obtained, but for unbalanced joint the two differential equations are coupled and the solution can only be obtained numerically.

In practical engineering design, simple and accurate analytical solutions are very useful because they can provide a relatively fast estimation of structural performance, particularly in the preliminary design stage. Subsequent finite element analyses or experimental investigations are not always necessary.

2. PRELIMINARY DIMENSIONING OF JOINTS BASED ON ANALYTIC RELATIONS

A pre-dimensioning algorithm will be presented by using the calculus relations deduced in paper [8] for balanced single-strap joints with thin adhesive layer (Fig.1). These relations will be rewritten in a more convenient form for the design purposes. The flexural stiffness of the two adherends is identical and the flexural stiffness of the overlap is about eight times greater.
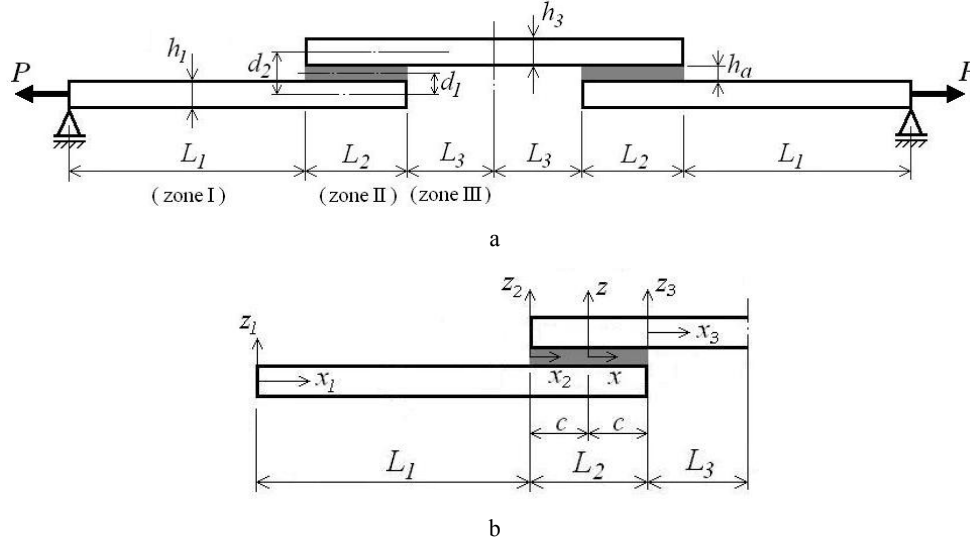

a

b

Fig. 1 – Geometry of single strapped joint with a gap between the ends of the adherends.

A preliminary evaluation of load capacity P (axial load per unit width) will be deduced in order to accomplish the strength conditions in some locations of the joint.

Allowable values are required for: a) combined tensile and bending maximum stress in the outher adherend, near the outer end of the overlap (zone I), b) combined tensile and bending maximum stress in the inner adherend (strap), at middle and near the inner end of the overlap (zone III), c) maximum equivalent stresses in adhesive (zone II), at the adhesive layer ends. The geometry that was considered (Fig. 1,a) permit to analyse cases when the overlap L_2 and the gap L_3 are small, mean or large. Figure 2 shows the typical deformed shape in case of a single-strapped joint. Because the dependence load-deflection is nonlinear, to establish the permitted load will be a relatively difficult task. Due to symmetry, the discussion that follows is referring to a half of the single-strapped joint on which local axes were considered for each zone (Fig. 1,b).

Fig. 2 – Deformed shape in case of a single-strapped joint.

In the mentioned development [8], concerning the balanced single-strapped joints, the adherends were modelled as cylindrical bending plates which have, on the three zones, the following stiffneses:

$$D_1 = D_3 = \frac{E h^3}{12\left(1-\nu^2\right)} = D; \qquad D_2 \approx \frac{E(2h)^3}{12\left(1-\nu^2\right)} = 8D, \qquad (1)$$

where $h = h_1 = h_3$ is the thickness of adherends which are made from a material having the elastic modulus E and the Poisson's ratio ν. A thin adhesive layer with thickness h_a ($h_a \ll h$) was considered.

Starting from the differential equations of elastic lines on the three zones of the joint the general expressions of deflections were deduced as:

$$w_1(x_1) = A_1 \cosh\left(\beta_1 x_1\right) + A_2 \sinh\left(\beta_1 x_1\right) \qquad (0 \le x_1 \le L_1), \qquad (2)$$

$$w_2(x_2) = A_3 \cosh\left(\beta_2 x_2\right) + A_4 \sinh\left(\beta_2 x_2\right) + d_1 \qquad (0 \le x_2 \le L_2), \qquad (3)$$

$$w_3(x_3) = A_5 \cosh(\beta_3 x_3) + A_6 \sinh(\beta_3 x_3) + d_2, \qquad (0 \le x_3 \le L_3), \tag{4}$$

where

$$\beta_k = \sqrt{\frac{P}{D_k}} \qquad (k = 1, 2, 3), \tag{5}$$

d_1 − distance between the middle planes of outer adherend and of adhesive layer, d_2 − distance between the neutral axes of the outer and inner adherends (Fig. 1a).

By imposing proper boundary and continuity conditions, i.e.

$$w_1(0) = 0; \qquad w_1(L_1) = w_2(0); \qquad \left.\frac{\mathrm{d}w_1}{\mathrm{d}x_1}\right|_{x_1=L_1} = \left.\frac{\mathrm{d}w_2}{\mathrm{d}x_2}\right|_{x_2=0}; \tag{6}$$

$$w_2(L_2) = w_3(0); \qquad \left.\frac{\mathrm{d}w_2}{\mathrm{d}x_2}\right|_{x_2=L_2} = \left.\frac{\mathrm{d}w_3}{\mathrm{d}x_3}\right|_{x_3=0}; \qquad \left.\frac{\mathrm{d}w_3}{\mathrm{d}x_3}\right|_{x_3=L_3} = 0, \tag{7}$$

were obtained the following expressions of the six integration constants:

$$A_1 = 0; \qquad A_2 = \frac{1}{B_3 \cosh(\beta_1 L_1)} \cdot \left[B_1 + d_1 \left(\frac{\beta_2}{\beta_1} \cdot \tanh(\beta_2 L_2) + \frac{\beta_3}{\beta_1} \cdot \tanh(\beta_3 L_3) \right) \right]; \tag{8}$$

$$A_3 = \frac{1}{B_3} \cdot \left[B_1 \cdot \tanh(\beta_1 L_1) - d_1 \left(1 + \frac{\beta_3}{\beta_2} \cdot \tanh(\beta_2 L_2) \cdot \tanh(\beta_3 L_3) \right) \right]; \tag{9}$$

$$A_4 = \frac{1}{B_3} \cdot \left[\frac{\beta_1}{\beta_2} \cdot B_1 + d_1 \left(\tanh(\beta_2 L_2) + \frac{\beta_3}{\beta_2} \cdot \tanh(\beta_3 L_3) \right) \right]; \tag{10}$$

$$A_5 = -\frac{1}{B_3} \cdot \left[(d_2 - d_1) \cdot B_2 + \frac{d_1}{\cosh(\beta_2 L_2)} \right]; \qquad A_6 = -A_5 \tanh(\beta_3 L_3), \tag{11}$$

where

$$B_1 = \frac{\beta_3}{\beta_1} \cdot \frac{\tanh(\beta_3 L_3)}{\cosh(\beta_2 L_2)} \cdot (d_2 - d_1); \qquad B_2 = 1 + \frac{\beta_2}{\beta_1} \cdot \tanh(\beta_1 L_1) \cdot \tanh(\beta_2 L_2); \tag{12}$$

$$B_3 = B_2 + \beta_3 \cdot \tanh(\beta_3 L_3) \cdot \left(\frac{\tanh(\beta_1 L_1)}{\beta_1} + \frac{\tanh(\beta_2 L_2)}{\beta_2} \right). \tag{13}$$

The main purpose of developing analytical solution was not predicting the lateral displacements of the joint, but to evaluate the bending moments and shear forces at the inner and outer ends of the overlap (M_i, V_i and M_0, V_0). Their expressions, in a condensed form, are

$$M_i = D_3 \cdot \left.\frac{\mathrm{d}^2 w_3}{\mathrm{d}x_3^2}\right|_{x_3=0} = P \cdot A_5; \qquad M_0 = D_1 \cdot \left.\frac{\mathrm{d}^2 w_1}{\mathrm{d}x_1^2}\right|_{x_1=L_1} = P \cdot A_2 \cdot \sinh(\beta_1 L_1); \tag{14}$$

$$V_i = D_3 \cdot \left.\frac{\mathrm{d}^3 w_3}{\mathrm{d}x_3^3}\right|_{x_3=0} = \beta_3 \cdot P \cdot A_6; \qquad V_0 = D_1 \cdot \left.\frac{\mathrm{d}^3 w_1}{\mathrm{d}x_1^3}\right|_{x_1=L_1} = \beta_1 \cdot P \cdot A_2 \cdot \cosh(\beta_1 L_1). \tag{15}$$

The distribution of shear and peeling stresses (τ and σ) in adhesive, along the overlap (where $-c \leq x \leq c$ and $c = L_2 / 2$), can be estimated by using the expressions [6, 8]

$$\tau = C_0 + C_1 \cosh(\lambda x) + C_2 \sinh(\lambda x) ; \tag{16}$$

$$\sigma = C_3 \cosh(\xi x)\cos(\xi x) + C_4 \cosh(\xi x)\sin(\xi x) + C_5 \sinh(\xi x)\cos(\xi x) + C_6 \sinh(\xi x)\sin(\xi x), \tag{17}$$

where

$$\lambda = \sqrt{\frac{G_a}{h_a} \cdot \left(\frac{2}{Eh} + \frac{h(h + h_a)}{2D}\right)} ; \qquad \xi = \sqrt[4]{\frac{E_a}{2 h_a D}} , \tag{18}$$

E_a and G_a are the tensile and the shear modules of the adhesive.

The values of constants C_i ($i = 0, 1, \ldots, 6$) will be calculated by using formulas

$$C_0 = \frac{P}{2c} - \frac{G_a}{2c\lambda^2 h_a} \cdot \left[\frac{2P}{Eh} + \frac{h}{2D} \cdot (M_o - M_i)\right] ; \tag{19}$$

$$C_1 = \frac{G_a}{\lambda h_a \sinh(\lambda c)} \cdot \left[\frac{P}{Eh} + \frac{h}{4D} \cdot (M_o - M_i)\right] ; \tag{20}$$

$$C_2 = -\frac{G_a}{\lambda h_a \cosh(\lambda c)} \frac{h}{4D} (M_o + M_i) ; \tag{21}$$

$$C_3 = \frac{E_a}{4D \ h_a B_4} \left[\xi(H_{SC} - H_{CS})(M_o - M_i) + H_{CC}(V_o + V_i)\right] ; \tag{22}$$

$$C_4 = \frac{E_a}{4D \ h_a B_5} \left[\xi(H_{CC} + H_{SS})(M_o + M_i) + H_{CS}(V_o - V_i)\right] ; \tag{23}$$

$$C_5 = \frac{E_a}{4D \ h_a B_5} \left[\xi(H_{CC} - H_{SS})(M_o + M_i) + H_{SC}(V_o - V_i)\right] ; \tag{24}$$

$$C_6 = \frac{E_a}{4Dh_a B_4} \left[\xi(H_{SC} + H_{CS})(M_o - M_i) + H_{SS}(V_o + V_i)\right] ; \tag{25}$$

where

$$B_4 = \xi^3 \left(\cos(\xi c)\sin(\xi c) + \cosh(\xi c)\sinh(\xi c)\right) ; \tag{26}$$

$$B_5 = \xi^3 \left(\cos(\xi c)\sin(\xi c) - \cosh(\xi c)\sinh(\xi c)\right) ; \tag{27}$$

$$H_{CC} = \cosh(\xi c)\cos(\xi c) ; \qquad H_{SS} = \sinh(\xi c)\sin(\xi c) ; \tag{28}$$

$$H_{CS} = \cosh(\xi c)\sin(\xi c) ; \qquad H_{SC} = \sinh(\xi c)\cos(\xi c) . \tag{29}$$

Starting from the values of shear and peel stresses in the critical point of the adhesive an equivalent stress can be calculated based on the criterion of energy of distortion (von Mises)

$$\sigma_{eq} = \sqrt{\sigma^2 + 3\tau^2} . \tag{30}$$

Following the design guide [11], the Hill's failure criterion will be applied to determine the maximum load that not induces damages in adhesive. The actual stress state is allowable in a point of the adhesive layer if is accomplished the condition

$$\chi = \left(\frac{\sigma}{\sigma_{fa}} \right)^2 + \left(\frac{\tau}{\tau_{fa}} \right)^2 \le 1, \tag{31}$$

where σ_{fa}, τ_{fa} are tensile and shear ultimate strengths of the adhesive.

Also, the strength condition for the adherends (zones I and III of the joint) can be written as

$$\max \left(\sigma_{max,I}, \sigma_{max,III} \right) \le \sigma_a, \tag{32}$$

where $\sigma_{max,I} = \frac{P}{h} + \frac{6 \ M_o}{h^2}$; $\sigma_{max,III} = \frac{P}{h} + \frac{6 \ |M_i|}{h^2}$, and σ_a is the allowable stress in the adherend material.

If the gap at the adherends ends is small (as example, if $L_3 < h/2$) significant discrepancies will be registered between the results, because the analytical formulas become inaccurate. Especially, the value of bending moment at the inner end of the overlap (M_i) and the maximum stresses in adhesive are affected [9].

3. COMPARISON BETWEEN ANALYTICAL AND NUMERICAL RESULTS

Results obtained by using the above presented relations will be compared with numerical ones, established by linear and nonlinear finite element analyses (FEA). Plane strain state and four node quadrilateral finite elements were used in the generation of numerical model. In order to validate the analytical model and to identify its limits of applicability, some numerical sets of joint geometric parameters were considered. In all cases was considered the structural adhesive AV 119 (also known as Araldite® 2007) which has the following elastic and strength characteristics: $E_a = 3,000$ MPa, $\nu_a = 0.35$, $\sigma_{fa} = 70$ MPa, $\tau_{fa} = 47$ MPa. The shear modulus was deduced based on the assumption that the adhesive is an isotropic material, i.e. $G_a = 0.5 \cdot E_a / (1 + \nu_a) = 1,110$ MPa.

First case which will be discussed is referring to a balanced single-strapped joint with aluminium adherends having the elastic modulus $E = 70,000$ MPa, the Poisson's ratio $\nu = 0.33$ and the allowable stress $\sigma_a = 180$ MPa. The applied axial load (per unit width), $P = 145$ N/mm, induces a nominal tensile stress of 50 MPa into the adherends. Dimensional parameters which were taken into account are: $L_1 = 80$ mm, $L_2 = 40$ mm, $L_3 = 10$ mm, $h = h_1 = h_2 = 2.9$ mm, $h_a = 0.2$ mm.

The values that are presented in Table 1 emphasize a good agreement between analytical and nonlinear elastic finite element analysis (NFEA) results. The linear elastic finite element analysis (LFEA) predicts correctly only the maximum equivalent stress in the outer adherend. Consequently, this kind of joint must be evaluated based on nonlinear analytical and numerical models.

The diagrams from Fig. 3 that present the distribution of shear and peel stresses in the adhesive emphasize a strong stress concentration at the inner ends of the overlaps and a less loaded portion (in the vicinity of the overlap middle). However, the main conclusion is that good predictions of maximum shear and peel stresses in adhesive can be made based on analytical calculus model.

Table 1

Comparison between analytical and numerical results

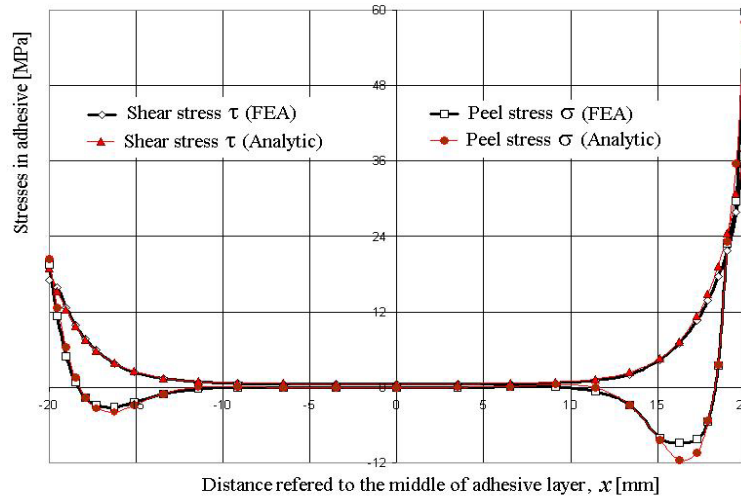| The calculus method	Maximum equivalent stresses in adherends [MPa]		Stresses at the inner ends of adhesive layers [MPa]			Maximum deflection [mm]
	Inner adherend	outer adherend	σ_{max}	τ_{max}	$\sigma_{eq,max}$	
Analytic	237	113	58	38	87.7	1.37
NFEA	240	135	59.7	39.5	85.5	1.54
LFEA	395	114	111	66	151	5.46

Fig. 3 – Distribution of shear and peel stresses along the adhesive layer, calculated analytically and by NFEA.

A short discussion of obtained analytical results from Table 1 is useful. Because the maximum equivalent stress in the inner adherend (of 237 MPa) exceeds the allowable stress ($\sigma_a = 180$ MPa), the study will be continued for an increased thickness of the strap. In a preliminary evaluation, this thickness can be taken as 1.5 times greater ($h_3 = 1.5 \cdot h = 4.35$ mm), while the thickness of outer adherends remains $h_1 = h = 2.9$ mm. On the other hand, starting from the shear and peel stresses in the critical zone of the adhesive, $\tau_{max} = 38$ MPa and $\sigma_{max} = 58$ MPa, an unacceptable value of the sum involved in the Hill's criterion was obtained: $\chi = 1.338 > 1$. Consequently, it is necessary to reduce the load. An approximate evaluation is possible based on the assumption that about the same reduction coefficient k is applied both to shear and peel stresses, as to obtain $\chi = 1$. From this condition was deduced that $k = 1/\sqrt{1.338} = 0.86$.

Taking into account the proposed modifications, i.e. $P = k \cdot 145 = 125$ N/mm and $h_3 = 4.35$ mm, a new NFEA was realised. The main results are the following:
- maximum equivalent stress in the inner adherend (strap), 170 MPa;
- maximum equivalent stress in the outer adherend, 92.4 MPa;
- maximum shear and peel stresses in adhesive, $\tau_{max} = 31.8$ MPa and $\sigma_{max} = 48.5$ MPa.

This solution is convenient because the strength conditions (31) and (32) are accomplished both for adherends and adhesive because $\sigma_{max,adher} = 170$ MPa $< \sigma_a$, $\chi = 0.937 < 1$.

4. EVALUATION OF LOAD CAPACITY OF SINGLE-STRAPPED JOINTS

The analytical model is associated to cases when adhesive does not exist in the middle zone of the joint (zone III in Fig. 1a). Analytical results are accurate if the length of gap between the adherends ends is greater than its thickness ($L_3 > h_1$). However, in many practical cases, the adherends are near ends and the gaps are completely or partially filled with adhesive.

The results which will be discussed in this section were obtained by NFEAs performed by using COSMOS/M Finite Element System [12]. Each nonlinear analyse was developed by applying the load in 100 steps. If the final loading is too great and induces stresses of unacceptable values in adhesive and/or in adherends, it is possible to identify the load capacity of the joint in a relatively simple manner: the load capacity is the maximum force which corresponds to a loading step where all strength conditions are accomplished.

In order to illustrate this procedure, the case of a single-strapped joint with unfilled gap was considered as: $L_1 = 80$ mm, $L_2 = 20$ mm, $L_3 = 0.2$ mm, $h_1 = 2.9$ mm, $h_3 = 3.5$ mm, $h_a = 0.2$ mm. The material properties were maintained as in the previous example. For intercomparative purposes, linear elastic and

nonlinear elastic finite element analyses were realised. It is to note that results obtained by LFEAs are overestimated with 10÷13% comparatively to those given by NFEAs. The total applied load was $P = 145$ N/mm, but, as show the results of nonlinear analysis from Table 2, the load capacity is of about $P/2$. The bold values emphasize that the strength conditions are accomplished if the load does not exceed 75 N/mm.

Table 2

Identification of load capacity in the case of a joint with unfilled gap (h_1 =2.9 mm, h_3 =3.5 mm, h_a =0.2 mm)

Number of loading step	Load N/mm	$\sigma_{eq,max}$ [MPa]		Stresses at the inner ends of adhesive layers [MPa]			w_{max} [mm]	χ
		Inner adherend	outer adherend	σ_{max}	τ_{max}	$\sigma_{eq,max}$		
20	29	72.8	18.0	21.3	10.7	28.2	0.114	0.144
40	58	142.6	35.3	41.4	21.0	55.1	0.185	0.549
50	72.5	**176.7**	43.7	51.2	26.0	68.2	0.215	**0.841**
60	87	210.4	52.0	60.9	31.0	81.2	0.241	1.192
80	116	276.5	68.2	79.6	40.7	106.3	0.289	2.042
100	145	341.2	84.0	97.9	50.2	130.9	0.331	3.096

If the load is imposed, a way to reduce the stresses induced in the components of the joint is to increase the thickness of the strap. Some NFEAs were made for single-strapped joints having dimensional parameters $L_1 = 80$ mm, $L_2 = 20$ mm, $L_3 = 0.2$ mm, $h_1 = 2.9$ mm and adherends from aluminium assembled by bonding with adhesive AV 119. The imposed load was $P = 145$ N/mm and the values of thickness of the strap which were taken into account are: 2.9 mm, 3.5 mm, 4.35 mm, 5.8 mm, 7.25 mm. The gap between the adherends ends was considered unfilled with adhesive. The diagrams from Fig. 4 show that the increment of strap thickness has a beneficial effect and for $h_3 \approx 6.4$ mm the strength condition (32) is accomplished. Also, the Hill's criterion is satisfied because the parameter χ is about equal to 1.
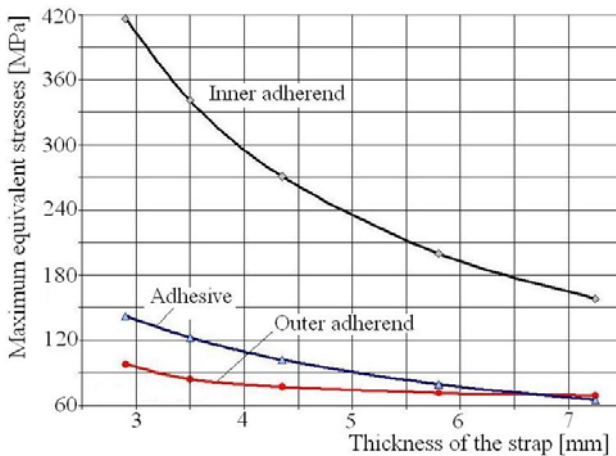

Fig. 4 – Influence of the strap thickness on the maximum stresses in the joint components.
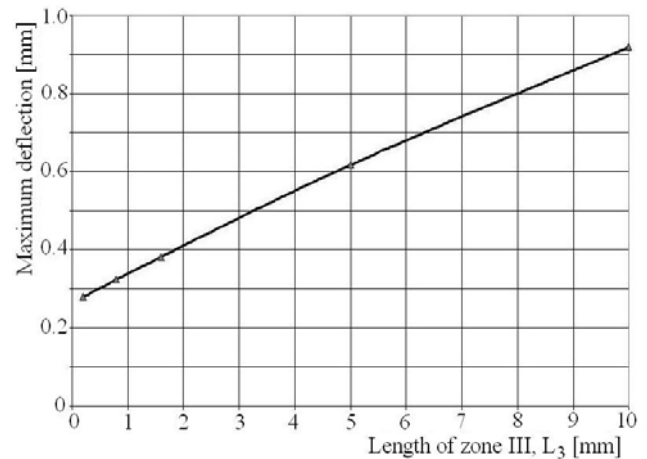
Fig. 5 – Influence of gap between the adherends ends on the maximum deflection (at the joint middle).

The influence of the gap length ($2L_3$) is also very important. Dependences of maximum lateral displacement (at the joint middle), of maximum stresses in the adherends and in the adhesive are emphasized in Figs. 5–7. These results were obtained for single-strapped joints with the geometry from Fig. 1a with the following fixed parameters: $P=72.5$ N/mm, $L_1 = 80$ mm, $L_2 = 20$ mm, $h_1 = h_3 = 2.9$ mm, $h_a = 0.2$ mm. The material properties were kept as in previous examples. The length of zone III was varied between 0.2 mm and 10 mm.
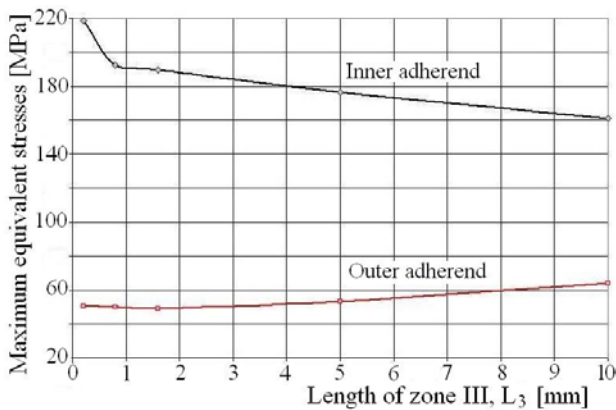
Fig. 6 – Influence of gap between the adherends ends on the maximum stresses in the adherends.
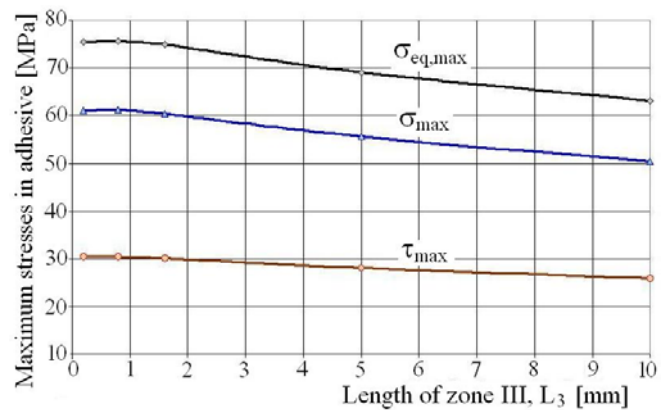
Fig. 7 – Influence of gap between the adherends ends on the maximum stresses in the adhesive.

It is interesting to study the case when the gap between the adherends ends is filled with adhesive. On the other hand, in practice, this fact is inherent if the length of zone III is short. The case with $P=145$ N/mm, $L_1 = 80$ mm, $L_2 = 20$ mm, $L_3 = 0.2$ mm, $h_1 = 2.9$ mm, $h_3 = 3.5$ mm, $h_a = 0.2$ mm was analysed both in the variants with unfilled and filled gap.

A great discrepancy between the behaviour of the two variants was found. The added adhesive has the desired effect, because a very important reduction of maximum peel and shear stresses in the basic adhesive layer is obtained, as is emphasized in Fig. 8. The diagrams present the distribution of shear and peel stresses along the adhesive layer, at the interface with the strap, where was identified the critical point, at the inner end of the overlap. The stresses were normalised by dividing them with the nominal tensile stress in the outer adherends $\sigma_n = P/h_1 = 50$ MPa. It is interesting that the maximum equivalent stress in the added adhesive is allowable, being of 36.9 MPa. The adhesive added in the gap permits to obtain a spectacular reduction of stress concentration in adhesive as an effect of diminution of bending moment acting in the inner adherend of the joint.
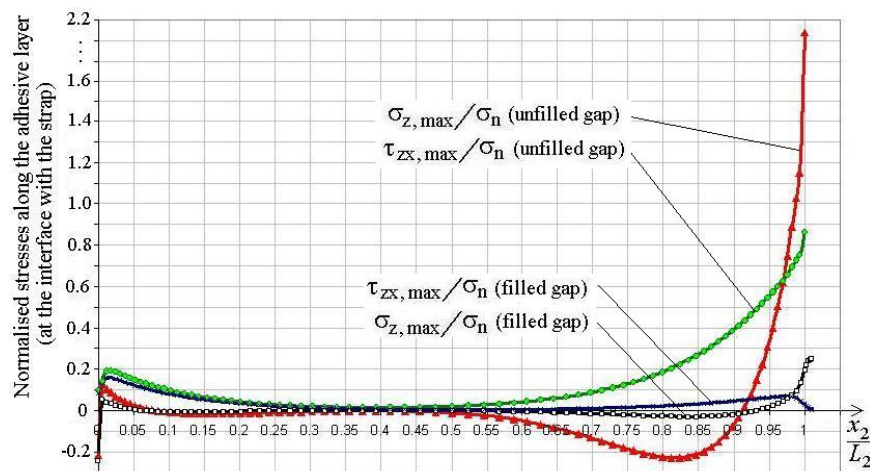

Fig. 8 – Variation of stresses in adhesive along the interface with the strap.

5. CONCLUSIONS

The nonlinear analytical model is very useful for pre-dimensioning the balanced single-strapped adhesive bonded joints, but the obtained results are accurate especially if the overlaps and the gaps between the ends of the adherends are relatively large. A good agreement between analytical and nonlinear elastic finite element analysis results was observed. The linear elastic finite element analysis predicts correctly only

the maximum equivalent stress in the outer adherend. Consequently, the behaviour of balanced or unbalanced single strapped joints in tension will be evaluated correctly if nonlinear analytical or numerical models will be used.

Based on the strength conditions described by using the von Mises and Hill criteria, a simple procedure to establish the load capacity in tension for single-strapped joints was presented in the paper.

For design purposes it is to underline that a spectacular improvement of strength performance of single strapped-joints with small gaps between the adherends ends can be obtained by filling the gap with adhesive and by using straps thicker than the outer adherends.

REFERENCES

1. ADAMS, R.D., COMYN, J., WAKE, W.C., *Structural adhesive joints in engineering*, London, Chapman & Hall, 1997.
2. DAVIES, M., BOND, D., *Principles and practice of adhesive bonded structural joints and repairs*, Int. Journal of Adhesion and Adhesives, **19**, pp. 91–105, 1999.
3. FAWAZ, S.A., DE RIJCK, J.J.M., *A thin-sheet, combined tension and bending specimen*, Experimental Mechanics, **39**, *3*, pp. 171–176, 1999.
4. HART-SMITH, L.J., *Designing to minimize peel stresses in adhesive bonded joints*, In "Delamination and debonding of materials" (Johnson W.S., editor), ASTM STP 876, pp. 238–266, 1885.
5. JARRY, E., SHENOI, R.A., *Performance of butt strap joints for marine applications*, Int. Journal of Adhesion and Adhesives, **26**, pp. 162–176, 2006.
6. LUO, O., TONG, L., *Closed-form solution for nonlinear analysis of single-sided bonded composite patch repairs*, AIAA Journal, **45**, *12*, pp. 2957–2965, 2007.
7. SANDU, M., SANDU, A., CONSTANTINESCU, D.M., SOROHAN ST., *The effect of geometry and material properties on the load capacity of single-strapped adhesive bonded joints*, Key Engineering Materials, **339**, pp. 89–96, Trans Tech Publications, Switzerland, 2009.
8. SHAHIN, K., TAHERI, F., *Analysis of deformations and stresses in balanced and unbalanced adhesively bonded single-strap joints*, Composite Structures, **81**, pp. 511–524, 2007.
9. TAHERI, F., ZOU, G.P., *Treatment of unsymmetric adhesively bonded composite sandwich panels-to-flange joints,* Mechanics of Advanced Materials and Structures, **11**, pp. 175–196, 2004.
10. TONG, L., *Strength of adhesively bonded single-lap and lap-shear joints*, Int. J. Solid Struct., **35**, *20*, pp. 2601–2616, 1998.
11. *   *   *   *Guide to the structural use of adhesives* (SETO), The Institution of Structural Engineers, London, 1999.
12. *   *   *   *COSMOS/M – Finite Element System, User Guide*, Structural Research & Analysis Corporation, USA, 1998.